

# How many groups? A statistical methodology for data-driven partitioning of infectious disease incidence into age-groups

Rami Yaari <sup>\*1,2</sup>, Amit Huppert <sup>†2,3</sup> and Itai Dattner<sup>‡1</sup>

<sup>1</sup>Department of Statistics, University of Haifa, Haifa, 34988, Israel

<sup>2</sup>Bio-statistical and Bio-mathematical Unit, The Gertner Institute for Epidemiology and Health Policy Research, Chaim Sheba Medical Center, Tel Hashomer, 52621, Israel

<sup>3</sup>School of Public Health, the Sackler Faculty of Medicine, Tel-Aviv University, Tel Aviv, 69978, Israel

## Abstract

Understanding age-group dynamics of infectious diseases is a fundamental issue for both scientific study and policymaking. Age-structure epidemic models were developed in order to study and improve our understanding of these dynamics. By fitting the models to incidence data of real outbreaks one can infer estimates of key epidemiological parameters. However, estimation of the transmission in an age-structured populations requires first to define the age-groups of interest. Mis-specification in representing the heterogeneity in the age-dependent transmission rates can potentially lead to biased estimation of parameters. We develop the first statistical, data-driven methodology for deciding on the best partition of incidence data into age-groups. The method employs a top-down hierarchical clustering algorithm, with a metric distance built for maximizing mathematical identifiability of the transmission matrix, and a stopping criteria based on significance testing. The methodology is tested using simulations showing good statistical properties. The methodology is then applied to influenza incidence data of 14 seasons in order to extract the significant age-group clusters in each season.

**Keywords:** epidemic modeling, parameter estimation, differential equations, clustering, multiple testing, influenza

---

<sup>\*</sup>ramiyaari@gmail.com

<sup>†</sup>amith@gertner.health.gov.il

<sup>‡</sup>idattner@stat.haifa.ac.il

# 1 Introduction

Infectious disease modeling has a long history dating back to the seminal works of Daniel Brenoulli on variolation of smallpox [1]. From a practical public health perspective, models are important in order to gain better understanding of the underlying mechanisms governing the disease dynamics. This in turn may lead to develop better control strategies to aid in the mitigation and elimination of the disease, and to predict the unfolding in real-time of outbreaks. In this work we focus on the deterministic SIR (susceptible - infected - removed) paradigm [2, 3, 4, 5] - a common paradigm upon which more sophisticated models are based.

An important empirical feature of many infectious diseases is the fact that the disease incidence is age-dependent. This observation has motivated the development of age-group models also known as age-stratified or age-structure models. These models employ an  $M \times M$  transmission matrix ( $M$  being the number of age-groups), known also as the WAIFW (Who Acquires Infection From Whom) matrix, describing the infection rates between the different groups [6, 7, 8, 9]. Ignoring the population age-structure can affect analysis results and potentially lead to biased estimation of parameters of interest. To illustrate the potential effect of age-groups on an outbreak dynamics, a somewhat trivial example is displayed in Figure 1. In this figure, the overall population incidence (which is an aggregation of the two distinct age-groups), can not be generated using a one-group SIR model (see Chapter 2.8.1 of [10]), and hence, a model lacking age-structure will not capture the observed dynamics, leading to a poor model fit and possibly biased inference.

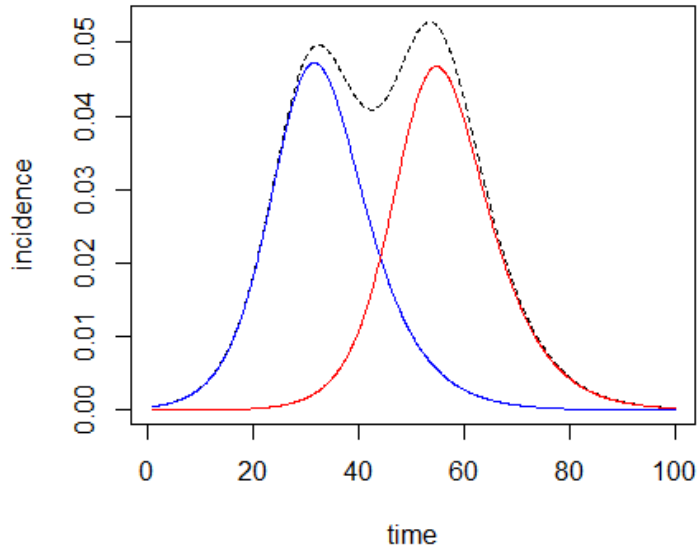
Parameter inference of mathematical epidemiological models is today a common practice [11] that requires fitting the models to real outbreak data [12, 13, 14, 15], a challenging task even in cases of low dimensional models [16]. Using recent advances in the area of parameter estimation for differential equations in general [17, 18], and for SIR models in particular [11, 19], it is possible to tackle the current problem of estimating parameters of a potentially large system of differential equations, which is a fundamental part of the problem of fitting age-group models. Specifically, [19] developed methodology for estimating directly the transmission matrix from incidence data without strong assumptions regarding the structure of the matrix.

However, estimation of the transmission matrix requires first to determine the age-groups of interest. Currently, to the best of our knowledge, there is no data-driven criterion on how to partition incidence data into age-groups. Existing practices to define the age-groups used for analyzing or modeling incidence data include: i) fixed age-group blocks (e.g., groups of 5 years), ii) administrative divisions (e.g., infants, toddlers, school children, etc) and iii) division based upon

age-dependent disease prevalence. The transmission matrix estimated using subjective or ad-hoc age-group partitioning can have an impact on both the perceived disease dynamics (see Figure 1) and on the estimates of key epidemiological parameters (e.g, the basic reproductive number  $R_0$ , defined as the mean number of infectives that a single case generates over the course of its infectious period in an entirely susceptible population). To overcome this gap we develop a statistical methodology for data-driven partitioning of infectious disease incidence into age-groups. The methodology is based on a criterion that will maximize mathematical identifiability of parameter estimation of the transmission matrix.

The paper is organized as follows. In Section 2 we formulate the problem and describe the statistical methodology; Section 3 presents the application of the method to simulated and real data, while a discussion is the subject of Section 4. Additional results are given in the Supplementary Material (SI).

Figure 1: Example of simulated incidence of two age-groups (blue and red solid curves) and their aggregated incidence (black dashed curve). The data was generated using model (1) with parameters:  $\beta = \begin{pmatrix} 1 & 0 \\ 0 & 1 \end{pmatrix}$ ,  $\gamma = 0.3$ ,  $N = (1, 1)$ ,  $S_0 = (0.5, 0.5)$ ,  $I_0 = (5 \times 10^{-4}, 5 \times 10^{-6})$ .



## 2 Methods

### 2.1 Problem definition

As mentioned above, a classical model used to describe the spread of a single outbreak in a population is the susceptible-infected-recovered (SIR) model. An age-group SIR model depicts the epidemic spread in different age-groups. A formulation of the model for  $j = 1, \dots, M$  age-groups, using an ordinary differential equation (ODE) system, is given by:

$$\begin{cases} S'_j(t) = -S_j(t) \sum_{k=1}^M \beta_{k,j} I_k(t) / N_k(t), \\ I'_j(t) = S_j(t) \sum_{k=1}^M \beta_{k,j} I_k(t) / N_k(t) - \gamma I_j(t), \\ R'_j(t) = \gamma I_j(t). \end{cases} \quad (1)$$

Here,  $\beta$  signifies the age-group transmission matrix, in which the element  $\beta_{k,j}$  is the infection transmission rate for an infective individual of age-group  $k$  and a susceptible individual of age-group  $j$ . The parameter  $\gamma$  is the recovery rate, which is assumed here to be the same for all age-groups, and  $N_j$  is the size of age-group  $j$ . The initial conditions for the system include the initial number of susceptibles  $S_{0j}$  and the initial number of infected  $I_{0j}$  in each age-group  $j$  (the number of recovered at any time is given by  $R_j(t) = N_j(t) - S_j(t) - I_j(t)$ , since the model assumes a closed population).

Typically, the incidence data  $I_j$  is observed with some noise while the number of susceptible individuals over time  $S_j$  is unknown. Assume that the observed incidence for each age-group  $j$  is obtained from the actual incidence according to the following statistical model (other statistical models can also be considered and employed in a similar scheme):

$$\tilde{I}_j(t) = I_j(t) + \epsilon_j, \quad \epsilon_j \sim N(0, \sigma_j^2), \quad j = 1, \dots, M, \quad t = 1, \dots, n. \quad (2)$$

Given noisy incidence curves  $\tilde{I}_j(t)$  for  $j = 1, \dots, M$  age-groups, constituting the most detailed description available of the incidence data in different age-groups, our goal is to find a partition of the incidence data into  $M_0 \leq M$  age-groups, that still allows estimating the age-group SIR model parameters, and in particular, the age-group transmission matrix  $\beta$ .

### 2.2 Partitioning algorithm

Here we describe the algorithm used to partition the incidence data into age-groups. The algorithm is based on a divisive (top-down) hierarchical clustering approach, where first a tree is built, representing a hierarchical partitioning of

the data into the most basic age-groups, and then the tree is pruned using a significance testing scheme. Since both the building and the pruning of the tree are based on the same criterion (given below), it is crucial that each of these steps (building and pruning) will be performed using a different data set generated from the same observed process. Multiple data sets for the same observed process can be obtained by dividing the incidence data into random sets (at the expense of some loss in statistical power, see Table 2 and Figure 2 below), or if there are multiple sources observing the same process (e.g., incidence data obtained from two different Health Maintenance Organizations (HMOs)). In the application to influenza data section below, we demonstrate another approach for obtaining multiple data sets. For now, let us assume that multiple data sets are given, so that we have noisy incidence data  $\tilde{I}_{j,k}(t)$  for  $t = 1, \dots, n$  time points,  $j = 1, \dots, M$  age-groups and  $k = 1, \dots, L$  sets, where it is assumed that  $\tilde{I}_{j,k}(t) = I_j(t) + \epsilon_{j,k}$  and  $\epsilon_{j,k} \sim N(0, \sigma_j^2)$  for all  $k = 1, \dots, L$ . We use half of the sets to build the tree and the other half to prune it.

To build the tree the algorithm starts with the incidence data of all age-groups summed together into a single time-series. We then test the  $M - 1$  possible ways to divide the incidence into two continuous age-group partitions,  $I_{a,k}$  and  $I_{b,k}$  (suppressing the notation of  $t$ ):

$$P_k : \quad I_{a,k} = \sum_{j=1}^k \tilde{I}_j, \quad I_{b,k} = \sum_{j=k+1}^M \tilde{I}_j.$$

For each candidate partition  $P_k, k = 1, \dots, M - 1$ , a statistic  $q_k$  is calculated using  $I_{a,k}$  and  $I_{b,k}$ . The statistic  $q_k$  will be used for deciding whether a partition should be made at this  $k$ . To be more specific, in a previous work [19], we have found that having two age-group incidence curves that are the same up to a factor, leads to mathematical non-identifiability of the transmission matrix. When the two curves are almost similar (up to a factor), the transmission matrix, while mathematically identifiable, would be practically non-identifiable. We therefore make use of this criterion as the basis for deciding how to separate the incidence data into age-groups. That is, a partition that gives rise to an identifiable model. For partition  $P_k$ , our null hypothesis  $H_{0,k}$  is that the two underlying incidence curves are the same up to a factor, meaning that  $I_{b,k}(\cdot) = cI_{a,k}(\cdot)$  for some constant  $c$ . We set  $d_k(t) = I_{b,k}(t) - \hat{c}I_{a,k}(t)$ , where  $\hat{c} = \sum_{t=1}^n I_{a,k}(t)I_{b,k}(t) / \sum_{t=1}^n (I_{a,k}(t))^2$ . Given the statistical model (2),  $\text{var}(d_k(t)) = \hat{c}^2\sigma_{a,k}^2 + \sigma_{b,k}^2 =: v_k$ , where  $\sigma_{a,k}^2 = \sum_{j=1}^k \sigma_j^2$  and  $\sigma_{b,k}^2 = \sum_{j=k+1}^M \sigma_j^2$ . The distance measure is then set as  $q_k := \frac{1}{v_k} \sum_{t=1}^n (d_k(t))^2$ . Under  $H_{0,k}$ , we have  $d_k(t) \sim N(0, v_k)$  for all  $t$  and therefore  $q_k \sim \chi^2(n)$ . Given partitions  $P_k, k = 1, \dots, M - 1$ , of  $I_{a,k}$  and  $I_{b,k}$ , we look for  $k$  that maximizes the

distance between the two groups:

$$\tilde{k} := \arg \max_{k=1, \dots, M-1} q_k, \quad (3)$$

and the selected partition is given by  $P_{\tilde{k}}$ . This procedure then repeats recursively until the data is partitioned completely. Note that in case  $\tilde{k}$  is not unique one can arbitrarily choose between them (however, we have not encountered such a scenario).

To prune the tree, we make another pass on the tree starting from its root. At each node, the statistic  $q_{\tilde{k}}$  is calculated for the now given partition  $P_{\tilde{k}}$  using the other half of the data set. We use the statistic  $q_{\tilde{k}}$  in a  $\chi^2$  test for the null hypothesis  $H_{0,\tilde{k}}$ . That is, for a given significance level  $\alpha \in (0, 1)$ , we will reject  $H_{0,\tilde{k}}$  if  $p = 1 - F_{\chi^2}(q_{\tilde{k}}, n) \leq \alpha$ . If the null hypothesis is not rejected, all child nodes of this node are pruned, meaning the incidence data at this node will be clustered together. Otherwise, the process continues with the child nodes. When the process stops, the leaves of the remaining pruned tree hold the clustering of the data.

Since we are performing multiple hypothesis tests during the pruning of the tree, we need to modify our significance level  $\alpha$  accordingly. We use the method described in [20] to control the familywise error rate (FWER) at level  $\alpha$  simultaneously across all nodes of the tree. At a given node that clusters  $m$  groups of the original  $M$  groups, the significance level according to [20] should be set as:  $\alpha^* = \frac{m}{M}\alpha$  (see also [21]). According to Theorem 1 of [20] this modification will ensure that the probability for rejecting the null hypothesis at each node will be smaller than  $\alpha$ . It means that in the root node, the significance level is  $\alpha$ , but as we proceed down the tree and get to finer and finer resolutions, the significance level becomes smaller, making it harder to partition the smaller clusters. We note that in order for Theorem 1 of [20] to hold in our case, we need monotonicity of p-values down the tree, which is guaranteed by our pruning procedure.

So far we have assumed that the variance parameters  $\sigma_1^2, \dots, \sigma_M^2$  are given. If they are not, they can be estimated from *all*  $L$  multiple data sets as  $\hat{\sigma}_j^2 = \frac{1}{n} \sum_{t=1}^n (s_j(t))^2$  where  $s_j(t) = \sqrt{\frac{1}{L-1} \sum_{k=1}^L (\tilde{I}_{j,k}(t) - \mu_j(t))^2}$  and where  $\mu_j(t) = \frac{1}{L} \sum_{k=1}^L \tilde{I}_{j,k}(t)$ . In the SI (section 1) we provide another approach for estimating the variance parameters  $\sigma_j^2$  and performing the clustering algorithm with only a single data set. Once we estimate the variance components from all  $L$  incidence curves, we can build and prune the tree as described above. Note that if  $L > 2$  and there are  $L' > 1$  data sets for building/pruning the tree, we would set  $\tilde{I}_j(t) = \frac{1}{L'} \sum_{k=1}^{L'} \tilde{I}_{j,k}(t)$  and modify  $\sigma_j^2$  to  $\sigma_j^2/L'$ .

Algorithms 2.1 and 2.2 provides a pseudo-code for the tree building and pruning procedures of the recursive partitioning algorithm, using one data set ( $X_1$ )

to build the tree and another one ( $X_2$ ) to prune it. The columns of the matrices  $X_1$  and  $X_2$  are the observed incidence belonging to the current node,  $\tilde{I}_1, \dots, \tilde{I}_m$ . Input vector  $V$  holds the noise parameters for the current node  $\sigma_1^2, \dots, \sigma_m^2$ . The output of the BuildTree procedure is the complete tree  $T$  which is given as input to the PruneTree procedure together with the total number of groups  $M$  and the significance level  $\alpha$  in order to produce the pruned tree. Figure S1 presents an example of a clustering tree produced by the algorithm before and after pruning. It should be noted that the two procedures can be performed in one cycle by first deciding how to partition the data and then performing the significance test to decide whether or not to do it.

---

**Algorithm 2.1:** BUILDTREE( $X_1, V$ )

---

```

 $T = \{\}$ 
 $n = \text{nrow}(X_1), m = \text{ncol}(X_1),$ 
if ( $m == 1$ )
  then  $T.k = 1$ ; return( $T$ )
 $q = []$ 
for  $k \in 1 : (m - 1)$ 
  do  $\begin{cases} V_a = \sum_{i=1}^k V[i], V_b = \sum_{i=k+1}^m V[i] \\ I_a = \sum_{i=1}^k X_1[, i], I_b = \sum_{i=k+1}^m X_1[, i] \\ c = \sum_{t=1}^n I_a(t)I_b(t) / \sum_{t=1}^n I_a(t)^2 \\ q[k] = \frac{1}{c^2 V_a + V_b} \sum_{t=1}^n (I_b(t) - cI_a(t))^2 \end{cases}$ 
 $\tilde{k} = \text{argmax}(q)$ 
 $V_a = V[1 : \tilde{k}], V_b = V[(\tilde{k} + 1) : m],$ 
 $X_a = X_1[, 1 : \tilde{k}], X_b = X_1[, (\tilde{k} + 1) : m],$ 
 $T.k = \tilde{k}$ 
 $T.a = \text{BuildTree}(X_a, V_a)$ 
 $T.b = \text{BuildTree}(X_b, V_b)$ 
return( $T$ )

```

---

---

**Algorithm 2.2:** PRUNETREE( $T, X_2, V, M, \alpha$ )

---

```

 $n = nrow(X_2), m = ncol(X_2),$ 
if ( $m == 1$ )
  then return( $T$ )
 $k = T.k$ 
 $V_a = \sum_{i=1}^k V[i], V_b = \sum_{i=k+1}^m V[i]$ 
 $I_a = \sum_{i=1}^k X_2[, i], I_b = \sum_{i=k+1}^m X_2[, i]$ 
 $c = \sum_{t=1}^n I_a(t)I_b(t) / \sum_{t=1}^n I_a(t)^2$ 
 $q = \frac{1}{c^2V_a+V_b} \sum_{t=1}^n (I_b(t) - cI_a(t))^2$ 
 $p = 1 - F_{\chi^2}(q, n)$ 
if ( $p \leq \frac{m}{M}\alpha$ )
  then  $\begin{cases} X_a = X_2[, 1 : k], X_b = X_2[, (k + 1) : m], \\ V_a = V[1 : k], V_b = V[(k + 1) : m], \\ T.a = PruneTree(T.a, X_a, V_a, M, \alpha) \\ T.b = PruneTree(T.b, X_b, V_b, M, \alpha) \end{cases}$ 
else  $T = NULL$  # meaning remove split
return( $T$ )

```

---

### 2.3 Verifying Type-I error and power of the algorithm

Monte-carlo simulations were used to test the Type-I error and power of the algorithm. We ran the age-group SIR model (1) to generate incidence data  $I_1, \dots, I_M$  where  $M = 20$  or  $M = 40$  groups. A diagonal age-group transmission matrix  $\beta$  was set to reflect various number of actual clusters  $M_0$ . For example, in order to generate incidence with a single cluster (i.e.,  $M_0 = 1$  clusters), all the diagonal components were set to the same value ( $\lambda = 0.84$ ) so that in actuality the same incidence is generated for all age-groups. To generate incidence with  $M = 20$  groups and  $M_0 = 4$  clusters, the diagonal was set to  $[\lambda, \lambda, \lambda, \lambda, \lambda, (1 - \delta) \cdot (\lambda, \lambda, \lambda, \lambda, \lambda), \lambda, \lambda, \lambda, \lambda, (1 - \delta) \cdot (\lambda, \lambda, \lambda, \lambda, \lambda)]$  with  $\delta > 0$ , so that in practice there are two different sets of incidence generated, separating the population into four distinct clusters (1-5,6-10,11-15,16-20). In all simulations, we set  $\gamma = 0.3$ ,  $N = 1$ ,  $S_0 = 0.5$ ,  $I_0 = 0.005$  for all  $M$  groups. The effective reproductive number (the expected number of infectives infected by a single infective in a partially susceptible population) of group  $j$  for which  $\beta_{j,j} = \lambda$  is  $R_{ej} = \frac{\lambda}{\gamma}S_0 = 0.84/0.3 \cdot 0.5 = 1.4$  [22]. The effective reproductive number of group  $k$  for which  $\beta_{k,k} = (1 - \delta) \cdot \lambda$  is  $R_{ek} = R_{ej} \cdot (1 - \delta)$ , implying that  $\delta$  represents the percentage difference in

$R_e$  between two age-group clusters. The number of observed time points in all simulations was set to  $n = 100$  and the significance level to  $\alpha = 0.05$ .

In the Monte Carlo study, 1000 sets of noisy incidence  $\tilde{I}_{1,k}, \dots, \tilde{I}_{M,k}$  with  $k = 1, \dots, L$  were generated from the incidence data  $I_1, \dots, I_M$  using the observation model (2) with the same  $\sigma_j$  for all  $j = 1, \dots, M$ . The values used for  $\sigma_j$  are given in Tables 1-2. We ran the partitioning algorithm on each set of 1000 simulations twice, once while assuming  $\sigma_j^2$  are known and once assuming they are unknown. When testing  $\alpha$  we recorded the number times the algorithm made a type-I error, *i.e.*, it rejected  $H_0$  and partitioned a cluster when it should not have. With  $M_0 = 1$  this means that the algorithm would reject  $H_0$  at the root node and split the incidence into more than a single cluster. With  $M_0 > 1$  this means that the algorithm would reject  $H_0$  at one of the nodes further down the tree representing an actual cluster.

To test the power of the algorithm we generated sets of 1000 simulations with varying values of  $\delta$ , and recorded the number of times the algorithm found the correct clustering. In addition, we calculated the adjusted Rand index (ARI) [23] for each simulation, measuring the similarity between the actual clustering and the algorithm's output clustering, and determined the mean ARI for each set of simulations. We also looked into the effect of increasing the number of observed incidence curves per age-group ( $L$ ) on the power of the algorithm.

## 2.4 Application to influenza incidence data

We applied our clustering methodology to daily incidence of influenza like-illness (ILI) diagnoses during 14 seasons (1998-2011). The diagnoses were given by physicians of the Maccabi Health Maintenance Organization (HMO) in Israel, which serves approximately 25% of the the Israeli population. The time period for each season was defined according to results of virological tests conducted on samples taken from patients visiting sentinel clinics. For the 2009 pandemic season we used only the period of the winter wave starting from October 2009. Prior to applying the algorithm, the incidences were smoothed using a 7-day moving average, to remove the weekly trend in the data. After smoothing, the number of days of incidence used per season varied between 71 days and 120 days, with a mean of 96 days and standard deviation of 13 days. In order to obtain multiple incidence data sets per age-group, we considered basic age-groups of 4-year bands, meaning that our basic age-groups were 0-3,4-7,8-11,...,60-63+, a total of  $M = 16$  groups. This assumes that the incidences within these age-groups are the same up to some noise (due to measurement error) and possibly scaling (due to differences in reporting rates). To address differences in scaling, we scaled each group of four incidence curves  $\tilde{I}_1, \tilde{I}_2, \tilde{I}_3, \tilde{I}_4$  by setting  $\check{I}_j(\tau) = \tilde{I}_j(\tau) \frac{\sum_{k=1}^4 \sum_{t=1}^n \tilde{I}_k(t)}{4 \times \sum_{t=1}^n \tilde{I}_j(t)}$ , for

$j = 1, 2, 3, 4$ ,  $\tau = 1, \dots, n$ . All four scaled incidences were used to estimate the per-group variance. We then used two of the incidences to build the hierarchical clustering tree and the other two incidences to prune the tree. For each season, we examined the results obtained using all six possible combinations for allocating the two incidences used for building and pruning the trees.

Finally, we fitted an age-group SIR model to each season of ILI data, clustered according to the clustering we found for that season, and estimated the transmission matrix  $\beta$  and the initial fraction of susceptible individuals in each age-group at the start of each season. A mean infection period of  $1/\gamma = 2.5$  days was fixed and the initial number of infected for each group was set according to the mean number of cases in the first three days of the season. In addition, a reporting rate of 10% was assumed across all age-groups and seasons. The fitting was performed using the R-package simode [24]. All code related to this work will be provided upon request, and will be uploaded to github in the near future.

## 3 Results

### 3.1 Simulations

Table 1 summarize the results of the simulations to verify type-I error. As can be seen, when  $\sigma_j^2$  are known, type-I error occurs less than  $\alpha = 0.05$  of the times, as expected. When  $\sigma_j^2$  are unknown and are estimated, the increase in the occurrences of type-I error are small. Table 2 summarizes the results of the power simulations. With a large enough  $\delta$  relative to the selected intermediate value of  $\sigma_j^2$ , the power of the algorithm is high. With  $\delta$  decreasing, the power decreases slowly until it falls off rapidly at some point, depending on the exact scenario. Estimating  $\sigma_j^2$  does not have a significant effect on the power. Increasing the number of incidence curves per age-group ( $L$ ) used as part of the clustering algorithm increases the power, as can be seen in Figure 2.

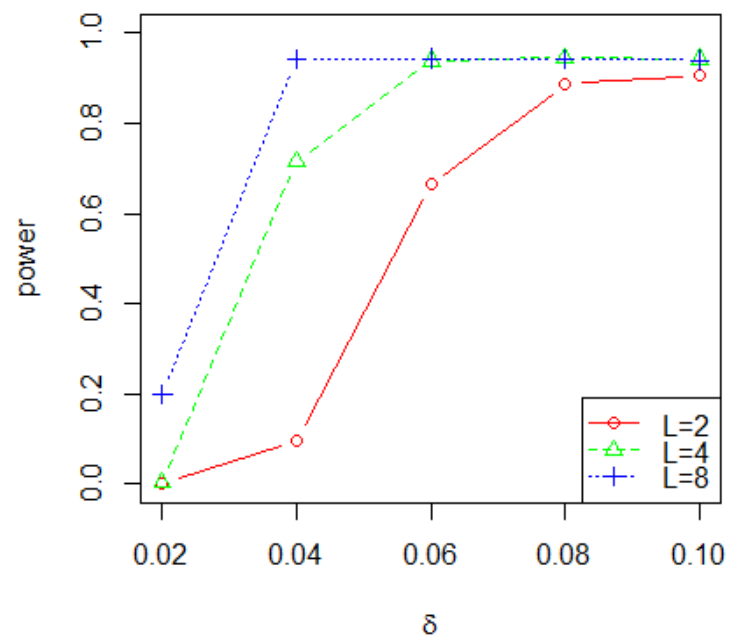
Table 1: Results of simulations to verify type-I error.  $M$  is the total number of age-groups.  $M_0$  is the number of clusters.  $\sigma_j$  are the noise parameters, set to be the same for each group in these simulations. The number of observed incidences per group was set to  $L = 2$  and significance level was  $\alpha = 0.05$ .

$M$	$M_0$	$\sigma_j^2$	$\sigma_j^2$ known	$\sigma_j^2$ unknown
			type-I error	
20	1	$10^{-6}$	0.033	0.054
		$10^{-5}$	0.034	0.054
	2	$10^{-6}$	0.037	0.053
		$10^{-5}$	0.037	0.057
	4	$10^{-6}$	0.035	0.046
		$10^{-5}$	0.037	0.048
40	1	$10^{-6}$	0.043	0.052
		$10^{-5}$	0.043	0.051
	2	$10^{-6}$	0.038	0.066
		$10^{-5}$	0.040	0.063
	4	$10^{-6}$	0.047	0.060
		$10^{-5}$	0.051	0.062

Table 2: Results of power simulations.  $M$  is the total number of age-groups.  $M_0$  is the number of clusters.  $\delta$  is the distance between clusters, measured as percentage difference in  $R_e$ . The noise parameters were set to  $\sigma_j^2 = 5 \times 10^{-6}$ . The number of observed incidences per group was set to  $L = 2$ .

$M$	$M_0$	$\delta$	$\sigma_j^2$ known		$\sigma_j^2$ unknown	
			power	mean ARI	power	mean ARI
20	2	0.01	0.248	0.422	0.242	0.427
		0.02	0.901	0.981	0.879	0.977
		0.03	0.961	0.993	0.941	0.990
		0.04	0.962	0.993	0.945	0.991
		0.05	0.962	0.993	0.945	0.991
	4	0.01	0	0.028	0	0.023
		0.02	0.091	0.329	0.088	0.326
		0.03	0.642	0.837	0.622	0.834
		0.04	0.896	0.981	0.889	0.982
		0.05	0.955	0.996	0.941	0.995
40	8	0.02	0	0.014	0	0.016
		0.04	0.124	0.363	0.116	0.360
		0.06	0.706	0.881	0.624	0.851
		0.08	0.924	0.986	0.889	0.981
		0.10	0.952	0.995	0.928	0.993
	2	0.01	0.503	0.860	0.491	0.858
		0.02	0.928	0.990	0.904	0.989
		0.03	0.958	0.994	0.935	0.992
		0.04	0.958	0.994	0.934	0.992
		0.05	0.958	0.994	0.936	0.992
	4	0.01	0	0.080	0	0.076
		0.02	0.404	0.763	0.389	0.760
		0.03	0.850	0.990	0.826	0.988
		0.04	0.928	0.996	0.912	0.996
		0.05	0.948	0.997	0.928	0.996
	8	0.02	0.004	0.088	0.001	0.088
		0.04	0.803	0.985	0.762	0.982
		0.06	0.947	0.998	0.936	0.998
		0.08	0.952	0.998	0.943	0.998
		0.10	0.953	0.998	0.944	0.998

Figure 2: Effect of the number of observed incidences per age-group ( $L$ ) on the power of the partitioning algorithm ( $M = 20$ ,  $M_0 = 8$ ,  $\sigma_j^2 = 5 \times 10^{-6}$ ).



### 3.2 Application: Seasonal Influenza

Figure 3 and Table 3 present the results of the clustering algorithm on age-group incidence of ILI collected during 14 seasons. The table also presents the first three partitions for each season according to their  $q_k$  statistic order, so that  $P_1$  represents the first and most significant partition,  $P_2$  the second and  $P_3$  the third. The results were obtained by running the algorithm six times for each season, each time using a different combination of incidences to build and prune the clustering tree (see Methods), and selecting the clustering that was the most in agreement with the other five clustering. The agreement of the selected clustering per season is also given in the table. It was calculated as the mean of the five pairwise ARI values. The full results of all six clustering per season are given in Table S3. In cases of a tie in the agreement of two different clustering, we selected the one with fewer clusters. While the six clustering per season had a lot in common, there were instances of notable variation. The agreement can therefore serve as a measure of confidence in the results of the clustering. The number of clusters obtained for all seasons range between two and six. In general, the most significant partition is between children and adults, with the mean age of  $P_1$  across all seasons being 17.1 (s.d. 2.9). In addition, children are frequently partitioned further into groups of younger and older children, while adults are only occasionally partitioned further, most notably around the age of 40. Figure 4 presents the age-group incidence of influenza in each season after the clustering. The incidences in the figure were normalized (each age-group incidence was divided by its sum) in order to allow to compare the incidences while ignoring differences in scaling.

Based on the clustering obtained above, the age-group SIR model (1) was fitted to the influenza incidence of each season. Figure 5 presents the obtained fits, and the estimated parameters are given in Table S4. The estimated transmission matrix  $\beta$  for each season has a dominant diagonal indicating that most of transmission occur within the age-groups. Using the estimated parameters we calculated the basic reproductive number  $R_0 = \frac{1}{\gamma} \rho(\mathcal{M}_0)$  and the effective reproductive number  $R_e = \frac{1}{\gamma} \rho(\mathcal{M}_e)$  for each season. Here,  $\beta_{ij} \frac{N_i}{N_j}$ , and  $S_{0i} \beta_{ij} \frac{N_i}{N_j}$  are the entries of the matrices  $\mathcal{M}_0$ , and  $\mathcal{M}_e$ , respectively, while  $\rho(A)$  is the spectral radius or maximum eigen value of matrix  $A$  [25]. The estimates of  $R_0$  and  $R_e$  as well as estimates of initial fraction of susceptibles in the whole population  $S_0 = \frac{\sum_{i=1}^m S_{0i} N_i}{\sum_{i=1}^m N_i}$ , are given in Table 4. In addition, for comparison, Table 4 presents estimates of  $R_0$ ,  $R_e$  and  $S_0$ , obtained by fitting an SIR model without age-groups to the observed incidence in the population as a whole. The estimates of  $R_0$  obtained from the model fits to the age-group incidence are typically higher than the estimates obtained from the fits to the incidence of the population as a whole, with mean  $R_0$  of 4.0 and 3.3 respectively (see also [22]).

Table 3: Age-group clusters obtained for each influenza season using the partitioning algorithm. The clustering given here is the one with the highest agreement (mean ARI) among the six clustering produced for each season by switching the incidences used to build the tree and pruning it (see text). Full results of all six clustering per season are given in table S3.  $P_1$ ,  $P_2$  and  $P_3$  are the age of the most, second most and third most significant partitions of the clustering, respectively, according the calculated  $q_k$  statistic.

season	clusters	agreement	$P_1$	$P_2$	$P_3$
1998	0-11, 12-15, 16+	0.97	12	16	-
1999	0-3, 4-11, 12-15, 16+	0.84	16	4	12
2000	0-7, 8-19, 20-39, 40+	0.90	20	8	40
2001	0-15, 16-23, 24-43, 44+	0.86	16	44	24
2002	0-15, 16+	0.89	16	-	-
2003	0-11, 12-15, 16-19, 20-35, 36+	0.94	20	12	36
2004	0-3, 4-15, 16+	0.83	16	4	-
2005	0-19, 20+	0.81	20	-	-
2006	0-3, 4-15, 16-19, 20-27, 28-43, 44-59, 60+	0.88	16	44	4
2007	0-3, 4-11, 12+	0.88	12	4	-
2008	0-19, 20-39, 40+	0.81	20	40	-
2009	0-3, 4-7, 8-11, 12-19, 20-51, 52+	0.96	20	8	52
2010	0-7, 8-11, 12-19, 20-27, 28-39, 40+	0.85	20	8	28
2011	0-3, 4-11, 12-15, 16+	0.99	16	4	12

Figure 3: Age-group clusters obtained for each of the 14 influenza seasons. This is a visualization of the results given in Table 3.

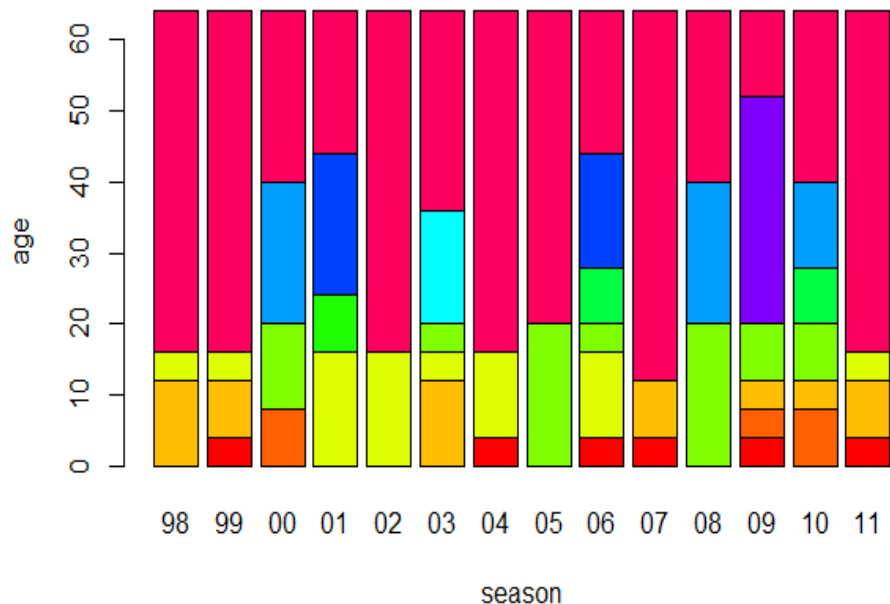


Figure 4: Clustered influenza incidence for each influenza season according to the results obtained using the partitioning algorithm. The incidences were normalized (each one divided by its sum) in order to present them in the same scale. The figures labeled ‘A’ show the mean incidence for each age-group cluster, while the figures labeled ‘B’ show all the age-group incidences, with incidences belonging to the same cluster appearing in the same color.

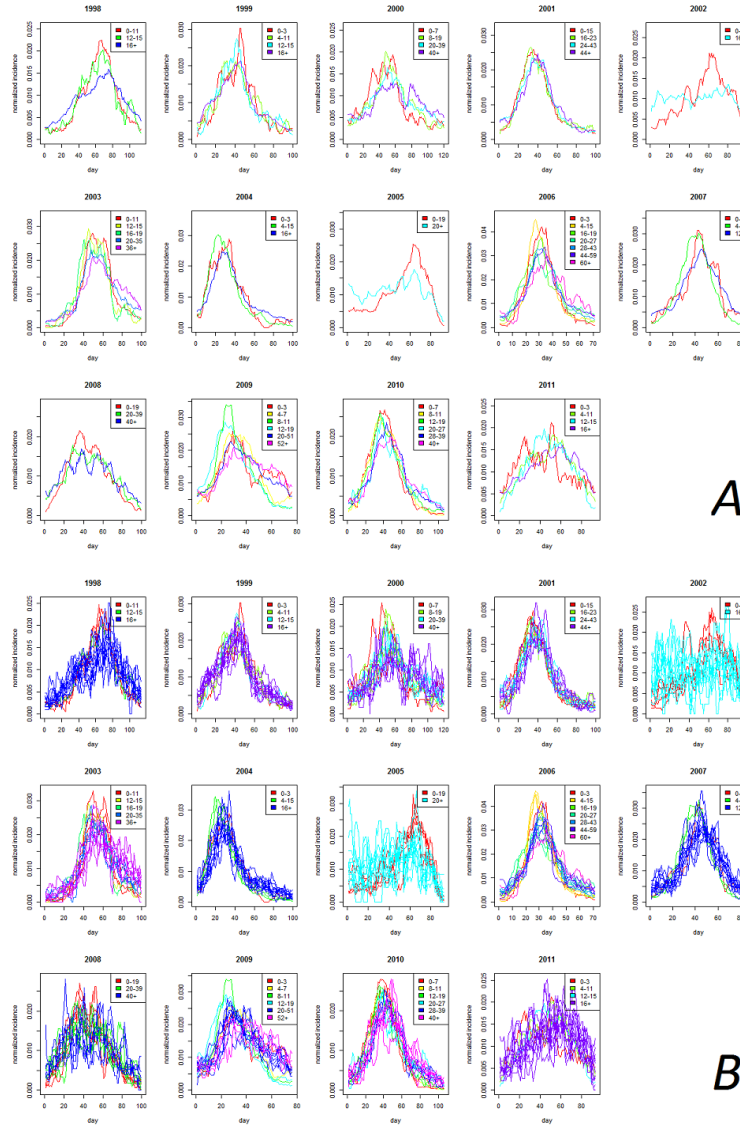


Figure 5: Model fits to clustered influenza incidence. The observed incidences are plotted using ‘+’ symbols while solid lines show the fits obtained by fitting model (1) to the data.

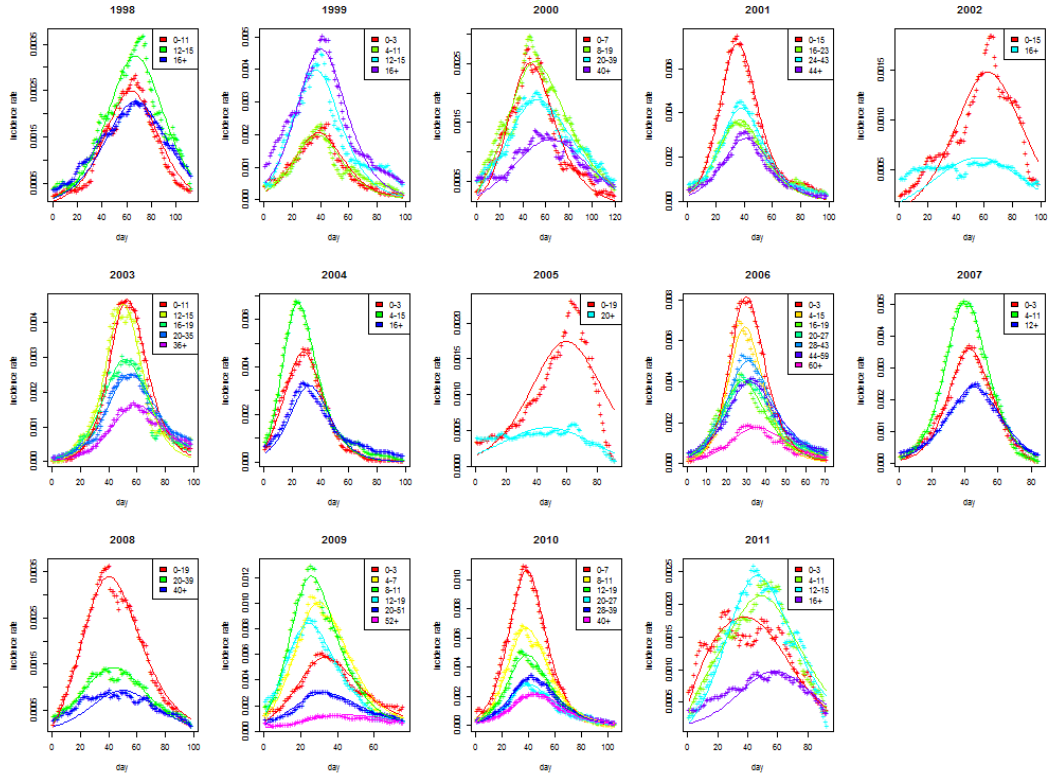


Table 4: Estimates of  $R_0$ ,  $R_e$  and  $S_0$  based on fitting an age-group model (AGM) to the clustered influenza incidence and fitting a model without age-groups to the incidence of the whole population (WPM).

season	$R_0$		$R_e$		$S_0$	
	AGM	WPM	AGM	WPM	AGM	WPM
1998	2.23	1.84	1.17	1.15	0.63	0.62
1999	3.11	2.31	1.21	1.22	0.56	0.53
2000	2.84	2.39	1.16	1.15	0.49	0.48
2001	3.03	2.72	1.26	1.27	0.47	0.47
2002	3.73	3.36	1.15	1.11	0.32	0.33
2003	3.91	3.81	1.31	1.24	0.43	0.33
2004	4.23	4.30	1.27	1.31	0.31	0.31
2005	7.78	3.69	1.15	1.12	0.24	0.30
2006	4.90	4.55	1.44	1.36	0.34	0.30
2007	3.81	3.71	1.31	1.24	0.33	0.33
2008	5.30	4.38	1.15	1.22	0.31	0.28
2009	2.84	2.63	1.23	1.26	0.52	0.48
2010	3.69	2.68	1.28	1.26	0.50	0.47
2011	4.77	3.58	1.15	1.15	0.33	0.32

## 4 Discussion

In this paper we develop a statistical methodology for data-driven partitioning of infectious disease incidence into age-groups. To the best of our knowledge this is a first attempt at this task. The methodology is based on explicit mathematical models describing infectious disease dynamics [26, 27, 28, 29, 30]. Specifically, we consider the case where there is a clear age-dependent dynamic. Our methodology uses a criterion of mathematical identifiability of parameter estimation of the transmission matrix, hence leading to "stable" models.

Mathematical models have proven to be an effective tool for examining and exploring the dynamics of the spread of infectious diseases [31, 32, 33, 34, 35]. In recent years, models have been applied in real-time as a supporting tool for decision makers to study and explore possible control and mitigation strategies [31, 32, 33, 34, 35]. However, previous age-dependent modeling studies did not use statistical methodology to stratify the population into age-groups. Using 'non-optimal' partitioning can lead to over simplified models, which can lead to biases in critical parameter estimations. For instance, Table 4 demonstrates that using 'simpler' models can lead to lower estimations of  $R_0$  which is a well known phenomena [22]. Such model miss-specifications can lead to critical mistakes in calculating the herd immunity required to mitigate an outbreak, which can lead to non-optimal decisions. On the other hand, employing too many age-groups unnecessarily, can lead to difficulties in parameter inference (due to a larger number of model parameters), identifiability issues, as well as computational difficulties.

The statistical methodology developed in this paper is based on significance testing in clustering, which addresses an important aspect of cluster validation [36]. As mentioned in the aforementioned book, many cluster analysis methods will deliver clusterings even for homogeneous data. They assume implicitly that a clustering has to be found, regardless of whether this is meaningful or not. Indeed, in our case one would like to know how to distinguish between a clustering that reflects meaningful heterogeneity in the data and not just an artificial clustering of homogeneous data. Significance tests are the standard statistical tools for such distinctions and therefore we adopt this approach. However, in view of the complexity of clustering problems, we prefer to consider the methodology developed here as a tool for data exploration with  $p$ -values used as a threshold supporting scientific reasoning (see, e.g., [37]). As such, the methodology allows to conduct a systematic data exploration of the partitioning.

The methodology outlined above is a top-down hierarchical clustering algorithm with a constraint on the type of divisions allowed and a statistically-based stopping criteria. The algorithm is designed to consider in a group only consecutive ages, hence enforcing a constraint on the partitioning. Thus, it is a semi-supervised

hierarchical clustering (i.e., clustering with knowledge-based constraints, see. e.g., [38, 39, 40]). Given the SIR model one could think of a model-based clustering [36]. Unfortunately, model based clustering in such a case requires to calculate maximum-likelihood of the data and therefore one would need to solve numerically the differential equations for all potential partitions, which is numerically and computationally challenging. Thus the methodology only uses the identifiability criterion for partitioning, which seems to capture the main characteristics of the underlying dynamics and lead to good statistical properties such as power and ARI.

The methodology as defined above is complete in the sense that we provide theoretical guarantees for it, and the assumptions underlying them are clearly posed. However, while we do provide a rigorous methodological structure, its current form is still limited. For example, consider Table 3 displaying the result of the method applied to the ILI data. A reasonable next step would be to explain the variance as seen in the results. It would be of epidemiological importance to test if the variability in age-group partitioning is an inherent property of influenza (e.g., due to the rapid evolution of the virus). Another explanation would be that we observe practical identifiability issues, meaning that several models are plausible given the data. Also, one may suggest to consider variability of  $S_0$  within groups (we assume they are the same). Such questions require further research. Finally, an additional interesting future research direction would be to apply the algorithm developed here for clustering spatial incidence. This might require modifications in the distance metric used here as well as other considerations which are beyond the scope of this work.

## Funding

This research was supported by the Israeli Science Foundation grant no. 387/15, and by a Grant from the GIF, the German-Israeli Foundation for Scientific Research and Development number I-2390-304.6/2015.

## References

- [1] Bernoulli D. Essai d'une nouvelle analyse de la mortalité causée par la petite vérole, et des avantages de l'inoculation pour la prévenir. *Histoire de l'Acad, Roy Sci(Paris) avec Mem.* 1760;p. 1–45.
- [2] Ross R. The prevention of malaria. John Murray; London; 1911.

- [3] Kermack WO, McKendrick AG. A contribution to the mathematical theory of epidemics. *Proceedings of the royal society of london Series A, Containing papers of a mathematical and physical character*. 1927;115(772):700–721.
- [4] Kermack WO, McKendrick AG. Contributions to the mathematical theory of epidemics. II. The problem of endemicity. *Proceedings of the Royal Society of London Series A, containing papers of a mathematical and physical character*. 1932;138(834):55–83.
- [5] Kermack WO, McKendrick AG. Contributions to the mathematical theory of epidemics. III. Further studies of the problem of endemicity. *Proceedings of the Royal Society of London Series A, Containing Papers of a Mathematical and Physical Character*. 1933;141(843):94–122.
- [6] Baguelin M, Hoschler K, Stanford E, Waight P, Hardelid P, Andrews N, et al. Age-specific incidence of A/H1N1 2009 influenza infection in England from sequential antibody prevalence data using likelihood-based estimation. *PLoS one*. 2011;6(2):e17074.
- [7] Ott J, Stevens G, Groeger J, Wiersma S. Global epidemiology of hepatitis B virus infection: new estimates of age-specific HBsAg seroprevalence and endemicity. *Vaccine*. 2012;30(12):2212–2219.
- [8] Anderson R, May R. Control of communicable diseases by age-specific immunisation schedules. *The Lancet*. 1982;319(8264):160.
- [9] Schenzle D. An age-structured model of pre-and post-vaccination measles transmission. *Mathematical Medicine and Biology: A Journal of the IMA*. 1984;1(2):169–191.
- [10] Banks RB. *Growth and Diffusion Phenomena: Mathematical Frameworks and Applications*. vol. 14. Springer Science & Business Media; 1993.
- [11] Dattner I, Huppert A. *Modern statistical tools for inference and prediction of infectious diseases using mathematical models*. SAGE Publications Sage UK: London, England; 2018.
- [12] Bolker BM. *Ecological models and data in R*. Princeton University Press; 2008.
- [13] Morton A, Finkenstädt BF. Discrete time modelling of disease incidence time series by using Markov chain Monte Carlo methods. *Journal of the Royal Statistical Society: Series C (Applied Statistics)*. 2005;54(3):575–594.

- [14] Ionides EL, Bretó C, King AA. Inference for nonlinear dynamical systems. *Proceedings of the National Academy of Sciences*. 2006;103(49):18438–18443.
- [15] Hooker G, Ellner SP, Roditi LDV, Earn DJ. Parameterizing state-space models for infectious disease dynamics by generalized profiling: measles in Ontario. *Journal of The Royal Society Interface*. 2010;8(60):961–974.
- [16] Voit EO, Almeida J. Decoupling dynamical systems for pathway identification from metabolic profiles. *Bioinformatics*. 2004;20(11):1670–1681.
- [17] Dattner I, Klaassen CA, et al. Optimal rate of direct estimators in systems of ordinary differential equations linear in functions of the parameters. *Electronic Journal of Statistics*. 2015;9(2):1939–1973.
- [18] Dattner I, Miller E, Petrenko M, Kadouri DE, Jurkevitch E, Huppert A. Modelling and parameter inference of predator–prey dynamics in heterogeneous environments using the direct integral approach. *Journal of The Royal Society Interface*. 2017;14(126):20160525.
- [19] Yaari R, Dattner I, Huppert A. A two-stage approach for estimating the parameters of an age-group epidemic model from incidence data. *Statistical Methods in Medical Research*. 2018;27(7):1999–2014. PMID: 29260611. Available from: <https://doi.org/10.1177/0962280217746443>.
- [20] Meinshausen N. Hierarchical testing of variable importance. *Biometrika*. 2008;95(2):265–278.
- [21] Kimes PK, Liu Y, Neil Hayes D, Marron JS. Statistical significance for hierarchical clustering. *Biometrics*. 2017;73(3):811–821.
- [22] Keeling M, Rohani P. *Modeling Infectious Diseases in Humans And Animals*. Princeton University Press; 2008.
- [23] Rand W. Objective Criteria for the Evaluation of Clustering Methods. *Journal of the American Statistical Association*. 1971;66(336):846–50.
- [24] Yaari R, Dattner I. *simode: R Package for statistical inference of ordinary differential equations using separable integral-matching*. arXiv preprint arXiv:180704202. 2018;.
- [25] Diekmann O, Heesterbeek J, Metz J. On the definition and the computation of the basic reproduction ratio  $R_0$  in models for infectious diseases in heterogeneous populations. *Journal of mathematical biology*. 1990;28(4):365–382.

- [26] Anderson RM, May RM. *Infectious diseases of humans: dynamics and control*. Oxford university press; 1992.
- [27] Keeling MJ, Rohani P. *Modeling infectious diseases in humans and animals*. Princeton University Press; 2011.
- [28] Grassly NC, Fraser C. Mathematical models of infectious disease transmission. *Nature Reviews Microbiology*. 2008;6(6):477.
- [29] Huppert A, Katriel G. Mathematical modelling and prediction in infectious disease epidemiology. *Clinical Microbiology and Infection*. 2013;19(11):999–1005.
- [30] Heesterbeek H, Anderson RM, Andreasen V, Bansal S, De Angelis D, Dye C, et al. Modeling infectious disease dynamics in the complex landscape of global health. *Science*. 2015;347(6227):aaa4339.
- [31] Ferguson NM, Donnelly CA, Anderson RM. The foot-and-mouth epidemic in Great Britain: pattern of spread and impact of interventions. *Science*. 2001;292(5519):1155–1160.
- [32] Keeling M, Woolhouse M, May R, Davies G, Grenfell B. Modelling vaccination strategies against foot-and-mouth disease. *Nature*. 2003;421(6919):136.
- [33] Lipsitch M, Cohen T, Cooper B, Robins JM, Ma S, James L, et al. Transmission dynamics and control of severe acute respiratory syndrome. *Science*. 2003;300(5627):1966–1970.
- [34] Earn DJ, He D, Loeb MB, Fonseca K, Lee BE, Dushoff J. Effects of school closure on incidence of pandemic influenza in Alberta, Canada. *Annals of internal medicine*. 2012;156(3):173–181.
- [35] Yaari R, Kaliner E, Grotto I, Katriel G, Moran-Gilad J, Sofer D, et al. Modeling the spread of polio in an IPV-vaccinated population: lessons learned from the 2013 silent outbreak in southern Israel. *BMC medicine*. 2016;14(1):95.
- [36] Hennig C, Meila M, Murtagh F, Rocci R. *Handbook of cluster analysis*. CRC Press; 2015.
- [37] Wasserstein RL, Schirm AL, Lazar NA. Moving to a World Beyond "p < 0.05". *The American Statistician*. 2019;73(sup1):1–19.
- [38] Zheng L, Li T. Semi-supervised hierarchical clustering. In: 2011 IEEE 11th International Conference on Data Mining. IEEE; 2011. p. 982–991.

- [39] Bade K, Nürnberg A. Creating a cluster hierarchy under constraints of a partially known hierarchy. In: Proceedings of the 2008 SIAM international conference on data mining. SIAM; 2008. p. 13–24.
- [40] Zhao H, Qi Z. Hierarchical agglomerative clustering with ordering constraints. In: 2010 Third International Conference on Knowledge Discovery and Data Mining. IEEE; 2010. p. 195–199.